

# A Solar Cell That Is Triggered by Sun and Rain

Qunwei Tang,\* Xiaopeng Wang, Peizhi Yang, and Benlin He

**Abstract:** All-weather solar cells are promising in solving the energy crisis. A flexible solar cell is presented that is triggered by combining an electron-enriched graphene electrode with a dye-sensitized solar cell. The new solar cell can be excited by incident light on sunny days and raindrops on rainy days, yielding an optimal solar-to-electric conversion efficiency of 6.53 % under AM 1.5 irradiation and current over microamps as well as a voltage of hundreds of microvolts by simulated raindrops. The formation of  $\pi$ -electron|cation electrical double-layer pseudocapacitors at graphene/raindrop interface is contributable to current and voltage outputs at switchable charging–discharging process. The new concept can guide the design of advanced all-weather solar cells.

Recent advances in energy-harvesting call for the rational design of advanced devices with unprecedented performance in transporting charges.<sup>[1–3]</sup> Solar cells are a commonly considered photoelectrochemical device that convert solar energy into electricity by complicated processes.<sup>[4–10]</sup> Although great achievements have been made since the discovery of various solar cells, there is still a remaining problem that the currently known solar cells can only be excited by sunlight on sunny days. In this fashion, the solar cells can not realize electricity output (current, voltage, power) on rainy days, or at least the electricity generation is relatively low. The crucial reason for this is that the origination of photogenerated electrons are created under incident light illumination. With an aim of markedly elevating electricity creation, all-weather solar cells are promising to meet the growing energy demands. To address this issue, we would like to develop a new solar cell by integrating an electron-enriched electrode for electric signal outputs on rainy days with a dye-sensitized solar cell (DSSC) for photoelectric conversion on sunny days. Graphene is a two-dimensional carbon layer having large delocalized  $\pi$ -electron systems, acting as Lewis bases in aqueous solution to form electron donor–acceptor complexes with positively charged ions.<sup>[11]</sup> Therefore, there has been widespread utilization of graphene as a robust absorbent for  $\text{Pb}^{\text{II}}$  ions and organic dye removal from aqueous solution,<sup>[12,13]</sup> in which graphene can

combine with heavy metal ions and organic dyes through Lewis acid–base interactions. Inspired by this, we would like to realize electricity generation by dropping raindrops on graphene film, because rain is a gigantic salt reservoir full of positively and negatively charged ions. The positively charged ions such as  $\text{Na}^+$ ,  $\text{Ca}^{2+}$ , and  $\text{NH}_4^+$  in raindrops can be adsorbed onto graphene surface by Lewis acid–base interactions to drive electron migration when dropping raindrops onto graphene surface, creating electrical  $\pi$ -electron|cation double-layer pseudocapacitors for current and potential output.<sup>[14]</sup> Our focus is placed on detecting current and potential signals by dropping rain droplets onto reduced graphene oxide (rGO) surface.

The bi-triggered solar cell was assembled on an indium tin oxide (ITO)-polyethylene terephthalate (PET) substrate by coating a  $\text{TiO}_2$  anode layer with thickness of around 10  $\mu\text{m}$ , sensitizing with 0.5 mM N719 dye, and an ITO-PET supported Pt ( $\text{Pt}_3\text{Ni}$  alloy) counter electrode (CE) for front irradiation and  $\text{Co}(\text{Ni})_{0.85}\text{Se}$  CE for rear irradiation. Subsequently the redox electrolyte having  $\text{I}^-/\text{I}_3^-$  couples was injected into the interspace between a  $\text{TiO}_2$  anode and a CE and the solar cell was sealed under hot press. The details on fabricating solar cells are demonstrated in the Supporting Information. The rGO film was prepared by filtrating GO colloid prepared by the traditional Hummers method, transferred to back side (PET layer) of ITO-PET substrate by a heat-pressing method (at 40 °C and 0.2 MPa for 10 min), and subsequently reduced with 5 wt % HI ethanol solution for 10 h. The final solar cell architectures that can be excited by sunlight and rain are shown in Figure 1 and the Supporting Information, Figure S1.

When irradiated under simulated sunlight (AM1.5, 100  $\text{mW cm}^{-2}$ ), the bi-triggering DSSCs with pristine Pt and  $\text{Pt}_3\text{Ni}$  alloy CEs can yield photoelectric conversion efficiencies of 5.98 % and 6.53 % under front ( $\text{TiO}_2$  side) irradiation, respectively. The detailed photovoltaic parameters are summarized in the Supporting Information, Table S1. The alloying effect between Pt and Ni can markedly increase electrolyte adsorption and enhance the catalytic activity toward  $\text{I}^-/\text{I}_3^-$  redox couples (Supporting Information, Figure S2), arising from the deviation of electrons from Ni to Pt,<sup>[4]</sup> creation of gigantic adsorption sites, and matching of work function to potential of  $\text{I}^-/\text{I}_3^-$  couples.<sup>[15]</sup> Apart from being excited by incident light under front irradiation, the new solar cell can also realize electricity generation from rear (CE) side. Owing to the strong reflection of metal CEs, the highly optical transparent  $\text{Co}_{0.85}\text{Se}$  and  $\text{Ni}_{0.85}\text{Se}$  are applicable in such rear-irradiated solar cell,<sup>[16,17]</sup> yielding efficiencies of 4.26 % and 4.09 %, respectively. Figure 2 shows  $J$ - $V$  curves of the bi-triggering DSSC under AM 1.5 irradiation as well as the optical transparency spectra of  $\text{Co}_{0.85}\text{Se}$  and  $\text{Ni}_{0.85}\text{Se}$  CEs.

On rainy days, the new solar cells can be reversed with rGO film upward, creating current and voltage outputs under

[\*] Prof. Q. Tang, X. Wang, Dr. B. He  
Institute of Materials Science and Engineering  
Ocean University of China, Qingdao 266100 (P.R. China)  
E-mail: tangqunwei@ouc.edu.cn

Prof. P. Yang  
Key Laboratory of Advanced Technique & Preparation for Renewable Energy Materials  
Ministry of Education, Yunnan Normal University  
Kunming 650500 (P.R. China)

Supporting information for this article can be found under:  
<http://dx.doi.org/10.1002/anie.201602114>.

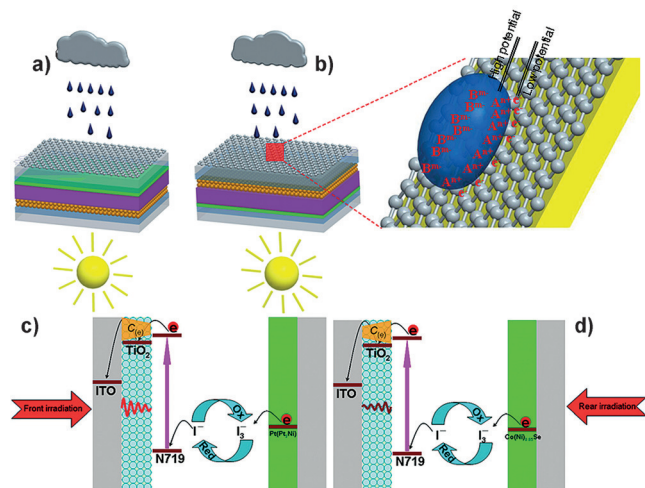


**Figure 1.** The bi-triggered flexible solar cell for recording photovoltaic performance under a) front or b) rear irradiation and measuring current and voltage signals by dropping raindrops (including  $A^{n+}$  and  $B^{m-}$  ions) onto rGO film. c), d) The operational principle of the flexible solar cell under sunlight. The rGO film is deposited on the PET side and solar cell is assembled on the ITO side. The two electrodes for measuring current and voltage signals in the presence of raindrops are coated with silver paint and subsequently protected with ethylene vinyl acetate copolymer. The droplets are injected by a medical syringe by controlling injection velocity.

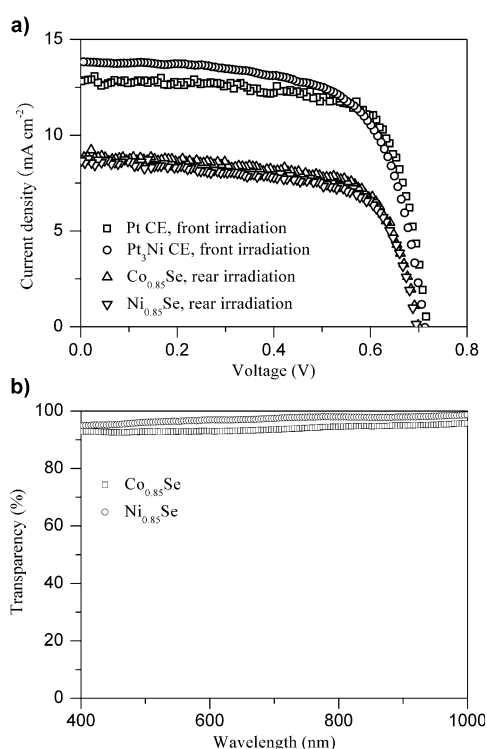


**Figure 2.** a)  $J$ - $V$  curves of the bi-triggering DSSC under AM 1.5 irradiation as well as b) optical transparency spectra of  $Co_{0.85}Se$  and  $Ni_{0.85}Se$  CEs.

the persistent dropping of raindrops (NaCl aqueous solution with concentration of 0.6 M, 1 M, or 2 M is used as simulated rain). The rGO film was characterized by Raman spectrum,

X-ray diffraction pattern (Supporting Information, Figure S3), and scanning electron microscopy (Supporting Information, Figure S4). A rGO strip with dimension of about  $20 \times 50 \text{ mm}^2$  was dropped by simulated raindrops, as shown in Figure 1. No signals for neither current nor voltage are detected without raindrops or using deionized water droplets (Supporting Information, Figure S5), while the current abruptly increases from nearly zero to  $0.29 \mu\text{A}$  within about 0.10 s when dropping a 0.6 M NaCl solution droplet, as shown in Figure 3 a. Subsequently, the current decreases back to zero in circa 0.83 s until the next signal. Notably, the current intensity can be further increased to 0.33 and  $0.54 \mu\text{A}$  by reducing the lateral distance between dropping point and electrode to 7.58 and 4.52 mm, respectively. Moreover, each droplet can yield voltage and output power of  $152.6 \mu\text{V}$  and  $7.17 \text{ pW}$  for 9.46 mm,  $54.7 \mu\text{V}$  and  $20.7 \text{ pW}$  for 7.58 mm, and  $25.1 \mu\text{V}$  and  $84.7 \text{ pW}$  for 4.52 mm, as shown in Figure 3 b,c. The time points for creating current are the same to that for voltage and output power, demonstrating the interaction between NaCl solution and rGO film. A potential mechanism behind these electric signals is the Lewis acid–base interaction. rGO is a two-dimensional system having a gigantic delocalized  $\pi$ -electrons as a result of  $sp^3$  hybridized C atoms,<sup>[18]</sup> therefore it is considered as a Lewis base in aqueous solution and can form  $\pi$ -electron|cation electrical double layer with Lewis acid such as  $Na^+$  ions. The pseudocapacitance at rGO/ionic solution interface is attributed to potential generation.<sup>[14]</sup> When dropping onto a rGO surface, simulated raindrops will quickly spread to the periphery. In this fashion, the cations are adsorbed at the front end, advancing the pseudocapacitor forward and drawing electrons in the rGO. The migration of drawing electrons creates current. Subsequently, the cations are desorbed at the rear end of the droplets during the shrinking process due to a hydrophobic rGO surface (Supporting Information, Figure S6a), discharging the pseudocapacitor and releasing the  $\pi$ -electrons to rGO. This discharging process results in a reduced current. Moreover, the final velocities of the droplets are calculated to be 30.8, 27.5, and  $21.3 \text{ cm s}^{-1}$  at lateral distances of 9.46, 7.58, and 4.52 mm, respectively. The induced voltage increases linearly with velocity of droplets (Supporting Information, Figure S7), agreeing with previous report.<sup>[14]</sup>

Apart from the lateral distance between dropping position and rGO, the time interval between two droplets controlled by injection velocity is also influential to electric signals. As shown in Figure 3 d–f, the signals produced at various injection velocities follow an order of  $20 \text{ mL h}^{-1}$  (ca.  $0.49 \mu\text{A}$ , ca.  $109.26 \mu\text{V}$ , ca.  $54.19 \text{ pW}$ )  $>$   $50 \text{ mL h}^{-1}$  (ca.  $0.37 \mu\text{A}$ , ca.  $44.48 \mu\text{V}$ , ca.  $20.63 \text{ pW}$ )  $>$   $80 \text{ mL h}^{-1}$  (ca.  $0.17 \mu\text{A}$ , ca.  $31.89 \mu\text{V}$ , ca.  $5.12 \text{ pW}$ ). The deep insight on the dependence of signal on time interval reveals that the rGO surface is of partial hydrophobicity due to a contact angle of  $92.4^\circ$  (Supporting Information, Figure S6a). In this fashion, some delocalized  $\pi$ -electrons in rGO may still be occupied by the  $Na^+$  in previous droplets at a high injection velocity. The reduced electrons result in reduced current and therefore  $\pi$ -electron|cation electric double-layer for voltage creation.

From electric double-layer theory, it is found that the current and voltage is highly dependent on ion concentration.

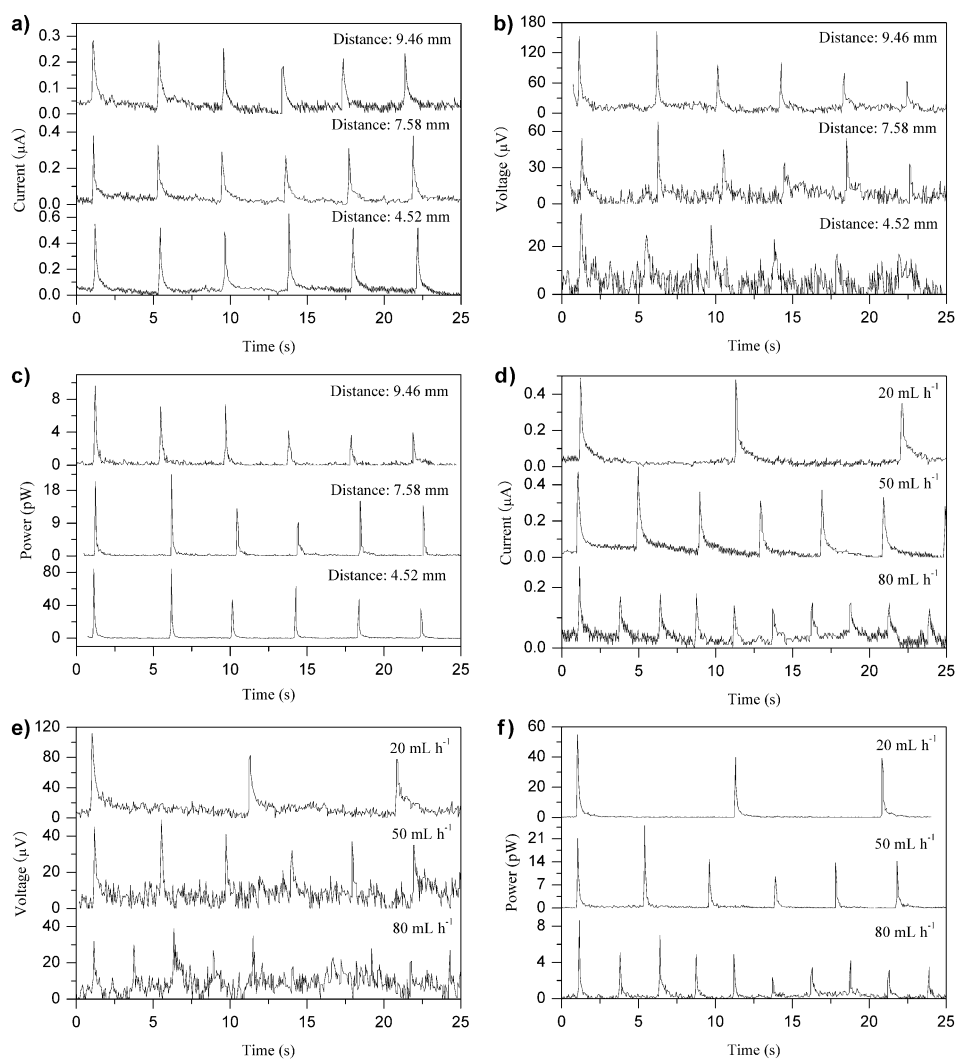


**Figure 3.** Current, voltage, and power signals produced by dropping 0.6 M NaCl solution droplets on rGO film at a)–c) different lateral distances between dropping point and rGO, and at d)–f) different time intervals of two droplets. The injection velocity and lateral distance are 50 mL h<sup>-1</sup> and 7.46 mm for recording (a) and (d), respectively.

By addressing this issue, we have compared the current and voltage created by dropping 2 M and 1 M NaCl aqueous solution as well as 0.6 M NaCl on the same rGO film, as shown in Figure 4 and the Supporting Information, Figures S8, and S9. Apparently, both current and voltage are markedly enhanced by increasing Na<sup>+</sup> concentration, yielding optimized values (ca. 0.82  $\mu$ A and ca. 84.76  $\mu$ V) at 2 M NaCl droplets. This result demonstrates that not all the delocalized  $\pi$ -electrons have formed  $\pi$ -electron|cation pseudocapacitance, but the unoccupied  $\pi$ -electrons can further interact with Na<sup>+</sup> at elevated concentration. Therefore, it is understandable that the potential difference for  $\pi$ -electron|cation pseudocapacitance is also enhanced at concentrated NaCl aqueous solution.

The long-term stability of this solar cell excited by sunlight and rain is more important than the actual value of signal. Here we have studied the performance evolution by persistently dropping 0.6 M NaCl droplets on rGO film over 1000 s at a time interval of 4 s. As shown in Figure 4c,d, 88.8 % or

initial current and 52.3 % of voltage are remained after repeatedly operation. A possible mechanism behind the deterioration is the partial hydrophobicity of rGO surface, thus it still susceptible to NaCl solution attack in either hydration of rGO with water (reduced static water contact angle in Figure S6b) or enlargement in interfacial resistance. The result is that partial occupied electrons are not released for the formation of  $\pi$ -electron|cation pseudocapacitance. Future optimization of designing highly hydrophobic graphene film with compact stacking is required to replace rGO for practical durability.

In summary, we have demonstrated a bi-triggering solar cell by integrating  $\pi$ -electron-enriched rGO film with a flexible DSSC device. The launched solar cells can be excited by sunlight on sunny days and raindrops on rainy days. Using metal and transparent metal selenide CEs, the solar cell can realize electricity generation under front and rear irradiation, respectively. Due to the formation of  $\pi$ -electron|cation pseudocapacitance at rGO/raindrop interface, current and voltage signals can be detected by dropping simulated rain droplets on rGO film. The preliminary results reveal that the signals are highly dependent on the lateral distance between dropping position and rGO, time interval of adjacent droplets, as well as Na<sup>+</sup> concentration, yielding maximal values (ca. 0.50  $\mu$ A, ca. 150  $\mu$ V, and ca. 50 pW). Moreover, the new device has a reasonable long-term stability, making it promising in creating electricity by raindrops. This work represents a significant step forward, as it opens a concept of developing all-weather solar cells that can persistently generate electricity in all weather.

### Acknowledgements

The authors acknowledge financial supports from National Natural Science Foundation of China (21503202, U1037604), Collaborative Innovation Center of Research and Development of Renewable Energy in the Southwest Area (05300205020516009), and Shandong Provincial Natural Science Foundation (ZR2011BQ017).

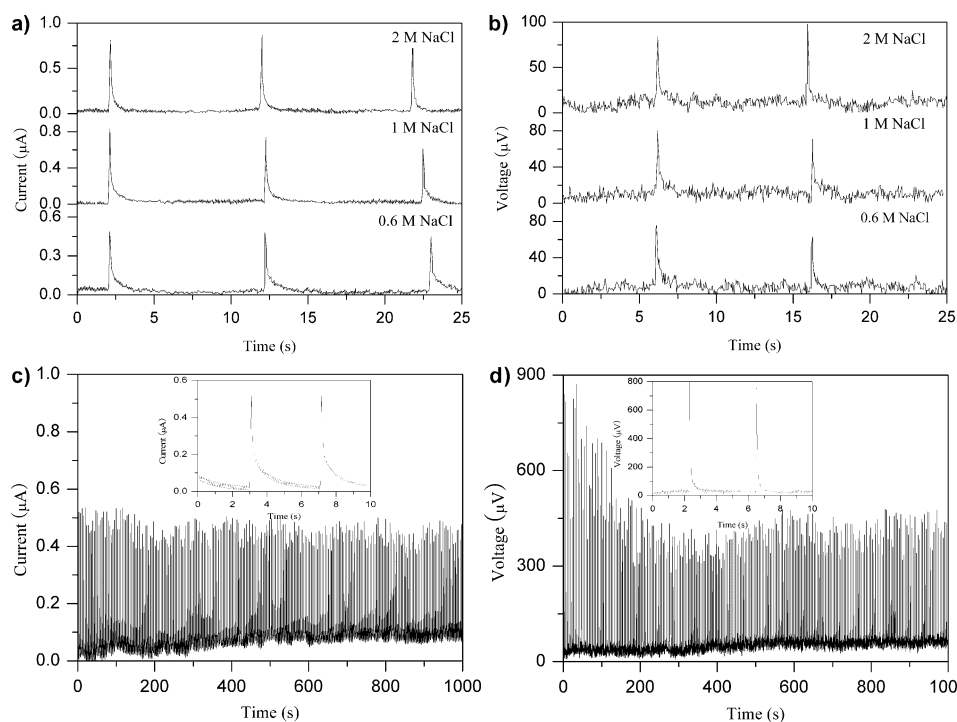


**Figure 4.** a) Current and b) voltage signals produced by dropping different droplets on rGO film. The injection velocity as well as lateral distance between dropping point and rGO are  $20 \text{ mL h}^{-1}$  and  $7.46 \text{ mm}$ , respectively. c) Current and d) voltage stability produced by persistently dropping  $0.6 \text{ M NaCl}$  solution droplets on rGO film. The injection velocity as well as distance between droplets and rGO are  $50 \text{ mL h}^{-1}$  and  $5 \text{ mm}$ , respectively.

**Keywords:** all-weather solar cells · counter electrodes · energy conversion · graphene electrodes

**How to cite:** *Angew. Chem. Int. Ed.* **2016**, *55*, 5243–5246  
*Angew. Chem.* **2016**, *128*, 5329–5332

- [1] N. Armaroli, V. Balzani, *Energy Environ. Sci.* **2011**, *4*, 3193–3222.
- [2] F. Zheng, C. H. Yang, X. Xiong, J. Xiong, R. Hu, Y. Chen, M. L. Liu, *Angew. Chem. Int. Ed.* **2015**, *54*, 13058–13062; *Angew. Chem.* **2015**, *127*, 13250–13254.
- [3] Q. H. Li, X. Jin, Y. Yang, H. Wang, H. Xu, Y. Cheng, T. Wei, Y. Qin, X. Luo, W. Sun, S. Luo, *Adv. Funct. Mater.* **2016**, *26*, 254–266.
- [4] Q. W. Tang, H. H. Zhang, Y. Y. Meng, B. L. He, L. M. Yu, *Angew. Chem. Int. Ed.* **2015**, *54*, 11448–11452; *Angew. Chem.* **2015**, *127*, 11610–11614.

- [5] N. J. Jeon, J. H. Noh, W. S. Yang, Y. C. Kim, S. Ryu, J. Seo, S. Seok II, *Nature* **2015**, *517*, 476–480.
- [6] W. Liu, W. Mu, Y. L. Deng, *Angew. Chem. Int. Ed.* **2014**, *53*, 13558–13562; *Angew. Chem.* **2014**, *126*, 13776–13780.
- [7] S. Friebe, B. Geppert, J. Caro, *Angew. Chem. Int. Ed.* **2015**, *54*, 7790–7794; *Angew. Chem.* **2015**, *127*, 7900–7904.
- [8] X. Jin, W. Sun, Z. Chen, T. Wei, C. Chen, X. He, Y. Yuan, Y. Li, Q. H. Li, *ACS Appl. Mater. Interfaces* **2014**, *6*, 8771–8781.
- [9] H. G. Jung, J. Hassoun, J. B. Park, Y. K. Sun, B. Scrosati, *Nat. Chem.* **2012**, *4*, 579–585.
- [10] T. Wang, J. L. Gong, *Angew. Chem. Int. Ed.* **2015**, *54*, 10718–10732; *Angew. Chem.* **2015**, *127*, 10866–10881.
- [11] L. R. Radovic, C. Moreno-Castilla, J. Rivera-Utrilla in *Chemistry and Physics of Carbon*, Vol. 27, Marcel Dekker, New York, **2001**, p. 227.
- [12] Z. H. Huang, X. Zheng, W. Lv, M. Wang, Q. H. Yang, F. Kang, *Langmuir* **2011**, *27*, 7558–7562.

- [13] Y. Yang, Y. Xie, L. Pang, M. Li, X. Song, J. Wen, H. Zhao, *Langmuir* **2013**, *29*, 10727–10736.
- [14] J. Yin, X. Li, J. Yu, Z. Zhang, J. Zhou, W. Guo, *Nat. Nanotechnol.* **2014**, *9*, 378–383.
- [15] Q. W. Tang, J. Liu, H. H. Zhang, B. L. He, L. M. Yu, *J. Power Sources* **2015**, *297*, 1–8.
- [16] Y. Y. Duan, Q. W. Tang, J. Liu, B. L. He, L. M. Yu, *Angew. Chem. Int. Ed.* **2014**, *53*, 14569–14574; *Angew. Chem.* **2014**, *126*, 14797–14802.
- [17] F. Gong, H. Wang, X. Xu, G. Zhou, Z. S. Wang, *J. Am. Chem. Soc.* **2012**, *134*, 10953–10958.
- [18] Q. Tang, Z. Zhou, Z. F. Chen, *Nanoscale* **2013**, *5*, 4541–4583.

Received: March 1, 2016

Published online: March 21, 2016